THE JOURNAL OF PHYSICAL CHEMISTRY A LETTERS

2008, *112,* 11965–11968
Published on Web 10/30/2008

Nonradiative Decay Mechanisms of the Biologically Relevant Tautomer of Guanine

Shohei Yamazaki,*,† Wolfgang Domcke,† and Andrzej L. Sobolewski‡

Department of Chemistry, Technical University of Munich, D-85747 Garching, Germany, and Institute of Physics, Polish Academy of Sciences, PL-02668 Warsaw, Poland

Received: July 25, 2008; Revised Manuscript Received: October 8, 2008

We present the excited-state potential energy profiles of the biologically relevant 9H-keto-amino tautomer of guanine with respect to the radiationless decay via the out-of-plane deformation of the six-membered ring as well as the dissociation of NH bonds. The CASPT2//CASSCF method is employed for the reaction-path calculations. The reaction path for the out-of-plane deformation in the $^1\pi\pi^*$ state leads in a barrierless way to a conical intersection with the electronic ground state. For the NH dissociation via the $^1\pi\sigma^*$ state, the 9H-keto-amino tautomer is shown to have lower energy barriers than the 7H tautomers which we have studied recently. These two radiationless decay mechanisms explain the unexpected missing of the biologically relevant form in the resonant two-photon ionization spectrum of guanine in a supersonic jet. It is suggested that these ultrafast deactivation processes provide the biologically relevant tautomer of guanine with a high degree of photostability.

It has been postulated that the DNA bases avail of particularly efficient mechanisms of radiationless deactivation after the absorption of UV light. Out-of-plane deformation of the six-membered ring in $^1\pi\pi^*$ states and dissociation of the NH bond in $^1\pi\sigma^*$ states have been proposed as reaction paths leading to conical intersections (CIs) of the S_1 and S_0 states. It is assumed that these ultrafast nonradiative decay mechanisms provide DNA with a high degree of photostability.[1−3]

The electronic spectra of isolated guanine in supersonic jets have been extensively studied using resonant two-photon ionization (R2PI) spectroscopy.[4−11] Guanine exhibits a complicated R2PI spectrum consisting of the overlapping spectra of at least four tautomers. Recent experiments[12−14] and reassignments of the spectra[11] have pointed out an intriguing feature in the R2PI spectrum of guanine: The biologically relevant 9H-keto-amino tautomer as well as the energetically most stable tautomer in the gas phase are missing in the R2PI spectrum, whereas energetically higher tautomers such as the 7H-enol-amino and 7H-keto-imino tautomers are detected. The missing of tautomers can be explained by the assumption that particularly fast radiationless decay processes render their excited-state lifetime too short to allow the detection of the R2PI signal.

A number of computational studies have been performed to provide insight into the photophysics of guanine tautomers. CIs of the out-of-plane-deformation type have been identified for several 9H and 7H tautomers.[15−20] For the 9H-keto-amino tautomer and several others, potential energy (PE) profiles leading to out-of-plane-type CIs have been calculated.[15,19]

Very recently, the present authors have performed a comparative investigation of the radiationless decay pathways of the S_1 state of the 7H-keto-amino, 7H-enol-amino, and 7H-keto-imino tautomers of guanine.[20] The out-of-plane deformation mechanism as well as the NH dissociation mechanism has been characterized with the complete-active-space self-consistent-field (CASSCF) method as well as second-order perturbation theory based on the CASSCF reference (CASPT2). The calculated PE profiles provide an explanation for the unexpected absence of the most stable 7H-keto-amino tautomer as well as the detection of the other 7H tautomers in the R2PI spectrum. In the present communication, we characterize the deactivation mechanisms of the biologically relevant 9H-keto-amino tautomer of guanine (Figure 1) in terms of the CASPT2//CASSCF energy profiles. The results provide evidence that the biologically relevant tautomer of guanine has the shortest excited-state lifetime of all guanine tautomers investigated so far.

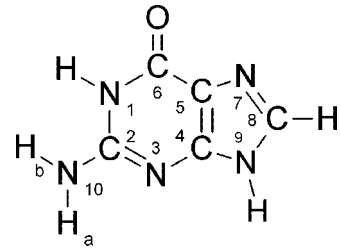

Figure 1. 9H-keto-amino tautomer of guanine.

The calculations were carried out with the MOLPRO[21] program package. Excited-state reaction paths and CIs between the ground state (S_0) and excited state (S_1) were optimized with the CASSCF method. For the calculation of reaction paths, one internal degree of freedom is chosen as the driving coordinate, while the energy is optimized with respect to all other internal coordinates. The out-of-plane deformation pathways were determined without any symmetry constraint, while the NH dissociation pathways were optimized with C_s symmetry restriction. Single-point internally contracted CASPT2 calculations[22] were performed at the optimized geometries to account for

* To whom correspondence should be addressed. E-mail: shohei.yamazaki@ch.tum.de.
† Technical University of Munich.
‡ Polish Academy of Sciences.

10.1021/jp806622m CCC: $40.75

TABLE 1: Vertical Excitation Energies (ΔE_{vert}), Oscillator Strengths (f), and Dipole Moments (μ) of the Ground State and the Low-Lying Singlet Excited States of the 9H-Keto-Amino Tautomer of Guanine, Obtained at the CASPT2//CASSCF Level with the Augmented Triple-ζ Basis Set

state	ΔE_{vert}/eV	f	μ/D
S_0			6.0
$^1\pi\pi^*$ (^1L_a)	4.51	0.164	5.6
$^1\pi\pi^*$ (^1L_b)	5.25	0.080	5.4
$^1n_o\pi^*$	5.22	0.001	3.8
$^1\pi\sigma^*$	4.89	0.005	11.8

dynamical electron correlation effects. A level shift with the parameter 0.3 was employed.[23] We used the (9s5p1d/4s1p)/[3s2p1d/2s1p] basis set[24] of double-ζ plus polarization quality and the (10s6p1d/5s1p)/[5s3p1d/3s1p] basis set[25] of triple-ζ plus polarization quality for the CASSCF and CASPT2 calculations, respectively. For the $^1\pi\sigma^*$ state, these basis sets were further augmented with diffuse basis functions.[24] We also calculated the CASPT2 vertical excitation energies at the ground-state equilibrium geometry. The latter has been determined with the second-order Møller−Plesset (MP2) method with the double-ζ plus polarization basis set. More details of the computational methods are given in the Supporting Information.

Table 1 gives the vertical excitation energies of the low-lying singlet excited states at the ground-state equilibrium geometry. The oscillator strengths and the CASSCF dipole moments are also included. The $^1\pi\pi^*$ state of ^1L_a character is the lowest excited state and has the largest oscillator strength among the states under consideration, which suggests that this $^1\pi\pi^*$ state is initially populated by photoabsorption. The lowest $^1n\pi^*$ state corresponds to the excitation from the lone pair orbital on the O atom. The $^1\pi\sigma^*$ state has a much larger dipole moment than the other states, due to the localization of charge in a diffuse σ^* orbital outside the molecular frame. The rather large dipole moment of the S_0 state of 9H-keto-amino guanine (6.0 D) is noteworthy. This large dipole moment stabilizes the highly polar $^1\pi\sigma^*$ state more than in the other tautomers of guanine.[18]

The vertical excitation energy of the ^1L_a state is in good agreement with previous CASPT2 and DFT/MRCI results.[15,18] The CC2 and EOMCCSD(T) methods yield a $^1\pi\pi^*$ excitation energy which is about 0.5 eV higher, as expected for these methods.[26,27] The CASPT2 energies of ref 19 are higher by about 0.4 eV due to the use of a rather restricted basis set (6-31G(d,p)). The $^1\pi\sigma^*$ state is only found among the lowest excited-states if a properly augmented basis set is used. [18,26]

Figure 2 shows the optimized geometries of two out-of-plane deformation type CIs, which connect the lowest $^1\pi\pi^*$ state with the ground state. The CIs in Figure 2, a and b, are referred to as $CI_{32}(1)$ and $CI_{32}(2)$, respectively. For both CIs, the six-membered ring undergoes a large out-of-plane deformation, characterized by a strong twisting of the N_3C_2 bond (see Figure 1 for the atom labeling). The relevant dihedral angle is $\delta(C_4N_3C_2N_1) = 69.0°$ and 72.5° at $CI_{32}(1)$ and $CI_{32}(2)$, respectively. The $^1\pi\pi^*$ state at these CIs is of biradical character. The dominant configuration corresponds to the excitation from the p orbitals localized mainly on N_3 and C_5 to that on C_2 (see Figure SI1 in the Supporting Information). The two CI_{32} structures correspond to different orientations of the N_1H bond. The dihedral angle $\delta(N_3C_2N_1H)$ is 81.1° at $CI_{32}(1)$ and 146.7° at $CI_{32}(2)$. In recent studies, the CIs corresponding to either $CI_{32}(1)$ or $CI_{32}(2)$ have been reported for the 9H-keto-amino tautomer. The CI structure obtained by Marian[18] is close to that

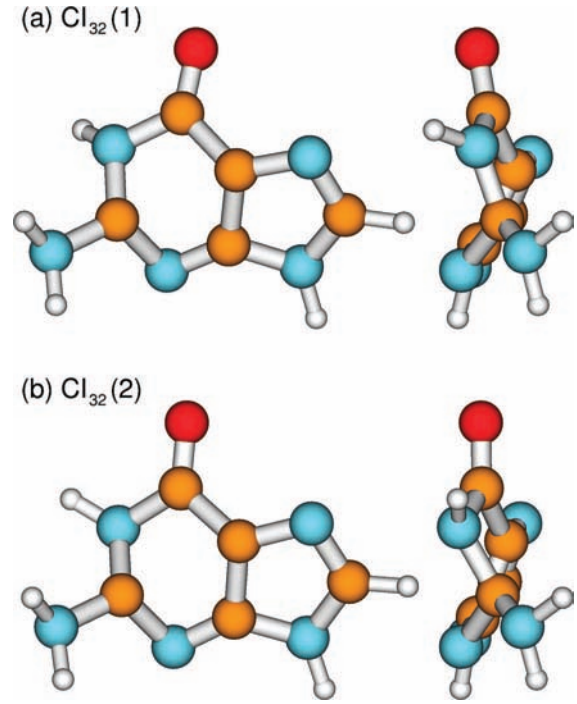

Figure 2. Optimized CI geometries of 9H-keto-amino guanine: (a) $CI_{32}(1)$ and (b) $CI_{32}(2)$.

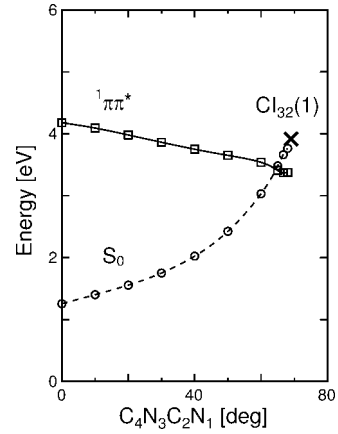

Figure 3. CASPT2 PE functions of the ground state (S_0; open circles) and the $^1\pi\pi^*$ state (open squares) of 9H-keto-amino tautomer of guanine along an out-of-plane deformation pathway leading to $CI_{32}(1)$. The full line indicates the $^1\pi\pi^*$ excited-state energies at the CASSCF-optimized geometries. The dashed line shows the ground-state energies at the $^1\pi\pi^*$ geometries. Cross indicates the CASPT2 energy at the CASSCF-optimized CI geometry.

of $CI_{32}(1)$. Chen and Li[15] and Serrano-Andrés et al.[19] reported a CI of a similar geometry as $CI_{32}(2)$.

We have calculated the excited-state PE functions leading to the CIs. The dihedral angle $\delta(C_4N_3C_2N_1)$ characterizing the CI_{32} structure was selected as the driving coordinate. The resulting CASPT2 energy profiles are shown in Figure 3. The full curve with open squares represents the energy profile of the $^1\pi\pi^*$ state along the reaction path. The dashed curve with circles gives the ground-state energies calculated at the $^1\pi\pi^*$-optimized geometries. The cross indicates the CASPT2 energy at the CASSCF-optimized $CI_{32}(1)$ structure. The reaction path starting at the Franck−Condon (FC) region results in a barrierless pathway toward $CI_{32}(1)$ and reaches a crossing with the ground state at about $\delta(C_4N_3C_2N_1) = 64°$. The energy of the crossing is estimated as 3.4 eV, which is 0.3 eV lower than the estimate of Chen and Li.[15] This result suggests that the 9H-keto-amino

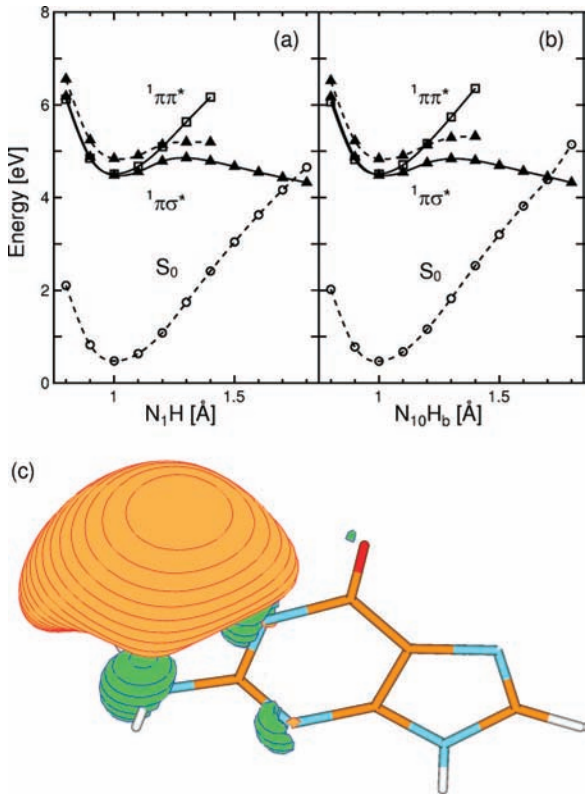

Figure 4. CASPT2 PE functions of the ground state (S_0; open circles), the $^1\pi\pi^*$ state (open squares), and the $^1\pi\sigma^*$ state (filled triangles) of 9H-keto-amino tautomer of guanine along dissociation pathways of NH bonds: (a) N_1H and (b) $N_{10}H_b$. The full lines indicate the excited-state energies calculated at their CASSCF-optimized geometries, and dashed lines show the ground-state energies at the $^1\pi\sigma^*$-optimized geometries and the $^1\pi\sigma^*$ state energies at the $^1\pi\pi^*$-optimized geometries. Panel c shows the σ^* orbital at the ground-state equilibrium geometry.

tautomer has an extremely short excited-state lifetime because of the barrierless radiationless decay through the CI, which can explain the absence of a R2PI signal for this tautomer. More details, including $CI_{32}(2)$ as well as the existence of PE minima close to these CIs, are discussed in the Supporting Information.

We have also calculated the reaction pathways for the NH dissociation of the 9H-keto-amino tautomer of guanine. Figure 4a,b shows the CASPT2 PE functions of the $^1\pi\pi^*$ and $^1\pi\sigma^*$ states as functions of the NH bond lengths. The length of the N_1H bond of the six-membered ring and the length of the $N_{10}H_b$ bond of the amino group were selected as the driving coordinates, because the diffuse σ^* orbital is covering these bonds at the ground-state geometry; see Figure 4c. The NH-stretching reaction paths were optimized in the $^1\pi\sigma^*$ states (full curves with triangles). The ground-state energies calculated at the $^1\pi\sigma^*$-optimized geometries (dashed curves with circles) and the $^1\pi\pi^*$ and $^1\pi\sigma^*$ energies calculated at the $^1\pi\pi^*$-optimized geometries (full curves with squares and dashed curves with triangles, respectively) are also shown in the figure. The $^1\pi\sigma^*$ energy functions are dissociative for both bonds, resulting in a crossing with the ground-state energy at a bond length of about 1.7 Å; see Figure 4a,b. The PE functions exhibit an energy barrier at a bond length of about 1.3 Å, reflecting the Rydberg-to-valence transformation of the σ^* orbital. The energy of the barrier top is estimated as 4.8 eV, which is about 0.3 eV above the vertical excitation energy of the ^1L_a state (4.51 eV).

At smaller values of the NH bond lengths, the $^1\pi\sigma^*$ energy functions are essentially degenerate with the $^1\pi\pi^*$ energy functions. Furthermore, the CASPT2 adiabatic excitation energy of the $^1\pi\sigma^*$ state (4.48 eV) is very close to the vertical excitation energy of the ^1L_a state. The DFT/MRCI calculation of Marian[18] predicted an even lower adiabatic excitation energy of the $^1\pi\sigma^*$ state (4.31 eV). It is therefore expected that the $^1\pi\sigma^*$ state can easily be populated by a nonadiabatic transition from the initially populated $^1\pi\pi^*$ state. It is worth noting that the 9H-keto-amino tautomer seems to have a lower barrier for dissociation via the $^1\pi\sigma^*$ state than all of the 7H tautomers considered so far.[20] The radiationless decay via the $^1\pi\sigma^*$ state is thus more efficient for the 9H-keto-amino tautomer than for other tautomers of guanine.

In a recent paper,[15] a much higher energy barrier was reported for the dissociation pathway of the N_1H bond, considering a highly out-of-plane deformed $^1\pi\pi^*$ minimum geometry as the starting point. However, this result does not exclude the possibility of the $^1\pi\sigma^*$ deactivation mechanism, because the $^1\pi\sigma^*$ state can be populated at nearly planar geometries, that is, before the onset of out-of-plane deformation. It is likely that the NH dissociation mechanism can compete effectively with the out-of-plane deformation mechanism, because of the small mass of the hydrogen atom. At the lowest excitation energies, the radiationless decay through the out-of-plane deformation pathway will presumably dominate the excited-state dynamics of 9H-keto-amino guanine.

In summary, the radiationless decay pathways of the biologically relevant 9H-keto-amino tautomer of guanine have been analyzed with computational methods, considering both the out-of-plane deformation and the NH dissociation mechanisms. This tautomer exhibits a barrierless excited-state pathway leading to an out-of-plane-deformation type CI with the ground state. The relative energy of the $^1\pi\sigma^*$ state and PE profile for NH dissociation indicate that the deactivation through the $^1\pi\sigma^*$ state is more likely for the 9H-keto-amino tautomer than for other tautomers of guanine. These findings strongly support the assumption that the 9H-keto-amino tautomer is missing in the R2PI spectrum due to ultrafast nonradiative excited-state deactivation through these particular pathways. The biologically relevant 9H-keto-amino tautomer seems to avail of the most efficient electronic deactivation mechanisms of all tautomers of guanine investigated so far.

Acknowledgment. This work has been supported by the Deutsche Forschungsgemeinschaft (DFG) through SFB 749. S.Y. acknowledges support by a fellowship of the Alexander von Humboldt Foundation. A.L.S. acknowledges partial support through a visitor grant of the DFG Cluster of Excellence "Munich-Centre for Advanced Photonics" (www.munich-photonics.de). We thank the Leibniz-Rechenzentrum der Bayerischen Akademie der Wissenschaften for substantial allocation of computing time.

Supporting Information Available: Computational details, additional results, Cartesian coordinates and drawings of energy minimum and conical intersection geometries, molecular orbitals at the conical intersection geometries, and additional potential energy profiles with respect to out-of-plane deformation pathways. This material is available free of charge via the Internet at http://pubs.acs.org.

References and Notes

(1) Crespo-Hernández, C. E.; Cohen, B.; Hare, P. M.; Kohler, B. *Chem. Rev.* **2004**, *104*, 1977.

(2) Abo-Riziq, A.; Grace, L.; Nir, E.; Kabelac, M.; Hobza, P.; de Vries, M. S. *Proc. Natl. Acad. Sci. U.S.A.* **2005**, *102*, 20.

(3) Sobolewski, A. L.; Domcke, W. *Europhys. News* **2006**, *37*, 20.
(4) Nir, E.; Grace, L.; Brauer, B.; de Vries, M. S. *J. Am. Chem. Soc.* **1999**, *121*, 4896.
(5) Nir, E.; Kleinermanns, K.; Grace, L.; de Vries, M. S. *J. Phys. Chem. A* **2001**, *105*, 5106.
(6) Nir, E.; Janzen, C.; Imhof, P.; Kleinermanns, K.; de Vries, M. S. *J. Chem. Phys.* **2001**, *115*, 4604.
(7) Piuzzi, F.; Mons, M.; Dimicoli, I.; Tardivel, B.; Zhao, Q. *Chem. Phys.* **2001**, *270*, 205.
(8) Mons, M.; Dimicoli, I.; Piuzzi, F.; Tardivel, B.; Elhanine, M. *J. Phys. Chem. A* **2002**, *106*, 5088.
(9) Chin, W.; Mons, M.; Dimicoli, I.; Piuzzi, F.; Tardivel, B.; Elhanine, M. *Eur. Phys J. D* **2002**, *20*, 347.
(10) Chin, W.; Mons, M.; Piuzzi, F.; Tardivel, B.; Dimicoli, I.; Gorb, L.; Leszczynski, J. *J. Phys. Chem. A* **2004**, *108*, 8237.
(11) Mons, M.; Piuzzi, F.; Dimicoli, I.; Gorb, L.; Leszczynski, J. *J. Phys. Chem. A* **2006**, *110*, 10921.
(12) Choi, M. Y.; Miller, R. E. *J. Am. Chem. Soc.* **2006**, *128*, 7320.
(13) Saigusa, H. *J. Photochem. Photobiol. C* **2006**, *7*, 197.
(14) Seefeld, K.; Brause, R.; Häber, T.; Kleinermanns, K. *J. Phys. Chem. A* **2007**, *111*, 6217.
(15) Chen, H.; Li, S. *J. Chem. Phys.* **2006**, *124*, 154315.
(16) Chen, H.; Li, S. *J. Phys. Chem. A* **2006**, *110*, 12360.
(17) Pugliesi, I.; Müller-Dethlefs, K. *J. Phys. Chem. A* **2006**, *110*, 13045.
(18) Marian, C. M. *J. Phys. Chem. A* **2007**, *111*, 1545.
(19) Serrano-Andrés, L.; Merchán, M.; Borin, A. C. *J. Am. Chem. Soc.* **2008**, *130*, 2473.
(20) Yamazaki, S.; Domcke, W. *J. Phys. Chem. A* **2008**, *112*, 7090.
(21) Werner, H.-J., et al., MOLPRO, version 2006.1, a package of ab initio programs; 2006; see http://www.molpro.net.
(22) Celani, P.; Werner, H.-J. *J. Chem. Phys.* **2000**, *112*, 5546.
(23) Roos, B. O.; Andersson, K. *Chem. Phys. Lett.* **1995**, *245*, 215.
(24) Dunning, T. H., Jr.; Hay, P. J. In *Methods of Electronic Structure Theory*, Schaefer, H. F., III, Ed.; Plenum: New York, 1977.
(25) Dunning, T. H., Jr. *J. Chem. Phys.* **1971**, *55*, 716.
(26) Fleig, T.; Knecht, S.; Hättig, C. *J. Phys. Chem. A* **2007**, *111*, 5482.
(27) Kowalski, K.; Valiev, M. *Res. Lett. Phys. Chem.* **2007**, doi: 10.1155/2007/85978.

JP806622M